HHS Public Access

Author manuscript

Alzheimers Dement. Author manuscript; available in PMC 2018 March 01.

Published in final edited form as:

Alzheimers Dement. 2017 March ; 13(3): 205–216. doi:10.1016/j.jalz.2016.08.005.

Defining imaging biomarker cut-points for brain aging and Alzheimer's disease

Clifford R. Jack Jr.[a,*], **Heather J. Wiste**[b], **Stephen D. Weigand**[b], **Terry M. Therneau**[b], **Val J. Lowe**[c], **David S. Knopman**[d], **Jeffrey L. Gunter**[e], **Matthew L. Senjem**[e], **David T. Jones**[d], **Kejal Kantarci**[a], **Mary M. Machulda**[f], **Michelle M. Mielke**[b], **Rosebud O. Roberts**[b], **Prashanthi Vemuri**[a], **Denise A. Reyes**[a], and **Ronald C. Petersen**[d]

[a]Department of Radiology, Mayo Clinic, Rochester, MN, USA

[b]Department of Health Sciences Research, Mayo Clinic, Rochester, MN, USA

[c]Department of Nuclear Medicine, Mayo Clinic, Rochester, MN, USA

[d]Department of Neurology, Mayo Clinic, Rochester, MN, USA

[e]Department of Information Technology, Mayo Clinic, Rochester, MN, USA

[f]Department of Psychiatry and Psychology, Mayo Clinic, Rochester, MN, USA

Abstract

INTRODUCTION—Our goal was to develop cut-points for amyloid PET, tau PET, FDG PET, and MRI cortical thickness.

METHODS—We examined five methods for determining cut-points.

RESULTS—The reliable worsening method produced a cut-point only for amyloid PET. The specificity, sensitivity, and accuracy of clinically impaired versus young clinically normal (CN) methods labeled the most people positive and all gave similar cut-points for tau PET, FDG PET and cortical thickness. Cut-points defined using the accuracy of clinically impaired versus age-matched CN method labeled fewer people positive.

DISCUSSION—In the future, we will employ a single cut-point for amyloid PET (SUVR 1.42, centiloid 19) based on the reliable worsening cut-point method. We will base lenient cut-points for tau PET, FDG PET and cortical thickness on the accuracy of clinically impaired vs young CN method and base conservative cut-points on the accuracy of clinically impaired vs age-matched CN method.

Keywords

Alzheimer's disease; Alzheimer's imaging; Alzheimer's MRI; amyloid PET; tau PET; FDG PET; Alzheimer's biomarkers; quantitative imaging

[*]Corresponding Author: Clifford R. Jack, Jr., MD, Department of Radiology, Mayo Clinic, 200 First Street SW, Rochester, MN 55905, Phone: 507-284-7096, Fax: 507-284-9778, jack.clifford@mayo.edu.

1. Background

Imaging and biofluid biomarkers of Alzheimer's disease (AD) are increasingly important to the study of brain aging and dementia. While every biomarker exists on a continuum, dichotomizing biomarker values is necessary in certain situations. Clinical trials require a positive/negative result when a biomarker is used to determine eligibility [1, 2]. Additionally, modern criteria for AD across the cognitive spectrum label individuals' biomarker positive or negative [3-7]. The goal of our study was to develop amyloid PET, tau PET, FDG PET, and structural MRI biomarker cut-points.

In brain aging and dementia research, defining a positive/negative cut-point for quantitative amyloid PET has received significant attention. Various methods have been used [8-15] including the 10^{th} percentile of clinically diagnosed AD dementia [16]. We adopted this last approach in 2012 [16] for amyloid PET, FDG PET and structural MRI with the assumption that the same method should be used to select cut-points for all biomarkers. However, we now believe that it may be appropriate to select cut-points for different AD biomarkers using different methods. In particular, it seems reasonable to treat amyloid biomarkers differently from others. Defining cut-points using individuals that meet certain clinical criteria without regard to evidence of amyloidosis is problematic [17]. The field has reached a consensus that biomarker evidence of amyloidosis is necessary for an accurate diagnosis of AD in living persons [3, 4, 6]. 10% −30% of individuals with clinically diagnosed AD dementia do not have AD at autopsy [18] or have no biomarker evidence of amyloidosis [19, 20]. Therefore, using a clinical diagnosis of AD dementia to define an "affected" group of case with AD when selecting biomarker cut-points has significant inherent error. Similarly, around 30% of clinically normal elderly individuals have AD at autopsy [21] or have biomarker evidence of amyloidosis [22-24] and therefore a clinically defined "unaffected" non-AD control group also has significant inherent error. [17]

Tau PET has recently been introduced [25-31] and defining a positive/negative cut-point is needed to place this modality on the same footing with other AD biomarkers. This in turn provides an opportunity to revisit the issue of defining cut-points for more established imaging biomarkers used in AD research. Our objective was to examine different methods for defining cut-points for amyloid PET, structural MRI, FDG PET, and tau PET. Identifying a single "best" cut-point for each biomarker would provide the most straightforward outcome. However, "best" depends on the context of use [32] and therefore it is reasonable that different cut-points might apply for a given biomarker when used for different purposes [33].

In practice, biomarkers vary in terms of whether numerically high or low values are more abnormal. To simplify our presentation, we have reversed the axes for FDG PET and corticalthickness so that from left to right values are increasing abnormal. In our general discussion of biomarkers, we treat higher values as more abnormal.

2. Methods

2.1. Participants

All clinically normal (CN) individuals in this study were participants enrolled in the Mayo Clinic Study of Aging (MCSA) [34]. Individuals with mild cognitive impairment (MCI) or AD dementia were participants enrolled in either the MCSA or the Mayo Alzheimer's Disease Research Center (ADRC). Beginning in 2004, the MCSA enrolled individuals aged 70 to 89 years; in 2012, the MCSA began enrolling individuals 50 plus years of age; and, in 2015 began enrolling individuals 30 plus years of age. From 2006 to 2015, the imaging battery consisted of MRI, FDG PET and amyloid PET. In 2015, tau PET was added to this battery and FDG PET became optional.

All individuals included in this study completed MRI and amyloid PET imaging. However, due to changes in the MCSA enrollment protocol, not all completed tau PET and FDG PET. Because of its recent introduction, only 401 individuals have tau PET scans. To take advantage of all available data, we created two separate samples for our analyses. The first sample included all individuals with tau PET, amyloid PET, and MRI (many of whom also had FDG PET). We refer to this sample as the "tau/amyloid/MRI sample." The second sample included all individuals with amyloid PET, FDG PET, and MRI. We refer to this sample as the "amyloid/FDG/MRI sample." Some of these individuals also had tau PET imaging. If individuals had multiple imaging visits, we used the first available visit with the necessary modalities.

The evolution of the MCSA described above has several practical implications. First, there are relatively few individuals under age 50. Since the start of tau PET scanning coincided with enrolling this younger age group, all who consented to imaging had tau PET, amyloid PET, and MRI. Second, serial imaging data are only available in individuals age 50 or over and only available for amyloid PET, FDG PET, and MRI.

2.2. Standard protocol approvals, registrations, and patient consents

These studies were approved by the Mayo Clinic and Olmsted Medical Center Institutional Review Boards and written informed consent was obtained from all participants.

2.3. Experimental design

2.3.1. Imaging methods—Amyloid PET imaging was performed with Pittsburgh Compound B [35] and tau PET with AV1451 [29]. CT was obtained for attenuation correction. Late uptake amyloid PET images were acquired from 40-60 minutes, FDG from 30-40 minutes, and tau PET from 80-100 minutes after injection. PET images were analyzed with our in-house fully automated image processing pipeline [36] where image voxel values are extracted from automatically labeled regions of interest (ROIs) propagated from an MRI template. An amyloid PET standardized uptake value ratio (SUVR) was formed from the voxel-number weighted average of the median uptake in the prefrontal, orbitofrontal, parietal, temporal, anterior and posterior cingulate and precuneus ROIs normalized to the cerebellar crus grey median. Amyloid PET values are expressed both in SUVR units and in centiloid units. The SUVR to centiloid conversion was done as recommended in Klunk et al

[37]. An AD-signature FDG PET composite or “meta-ROI” was formed from the voxel-number weighted average of the median uptake in the angular gyrus, posterior cingulate, and inferior temporal cortical ROIs and normalized to the pons and vermis median [38]. A tau PET meta-ROI was formed from a voxel-number weighted average of the median uptake in the entorhinal, amygdala, parahippocampal, fusiform, inferior temporal, and middle temporal ROIs normalized to the cerebellar crus grey median. PET data was not partial volume corrected. However, the data was “sharpened” - i.e. voxels whose probability of being CSF was greater than the probability of being grey matter and greater than the probability of being white matter were discarded from all PET ROI measures.

MRI was performed on one of three 3T GE systems. The MRI measure was a FreeSurfer (v5.3) derived AD-signature meta-ROI composed of the surface-area weighted average of the mean cortical thickness in the following individual ROIs: entorhinal, inferior temporal, middle temporal, and fusiform.

2.4. Statistical analysis

2.4.1. Methods of defining cut-points—We used five methods for determining biomarker cut-points which we term (1) reliable worsening, (2) specificity, (3) sensitivity, (4) accuracy of cognitively impaired versus younger CN, and (5) accuracy of cognitively impaired versus age-matched CN. We summarize the five methods graphically in Fig. 1 and describe the methodology in detail below.

The reliable worsening cut-point was based on identifying a threshold baseline value beyond which the rate of change in that biomarker worsens reliably. With this method, we first estimated the annual rate of change in each biomarker within each individual with serial imaging data using linear regression. Next, a nonparametric scatter plot smoother was used to plot the mean rate of change in biomarker on the y-axis versus the baseline biomarker value on the x-axis [39]. We then identified the biomarker value that corresponded to the minimum point on this rate vs baseline curve. While the minimum corresponds to a threshold beyond which the biomarker rate of change can be expected to increase on average, we obtained a more conservative, or reliable, cut-point by projecting the upper bound of a 50% prediction interval at the minimum rightward until it intersected the rate versus baseline curve. The point of this intersection defined a reliable worsening cut-point. Because we do not yet have longitudinal tau PET data, this reliable worsening analysis was only applicable to MRI, amyloid and FDG PET; and, as shown in results produced a result only for amyloid PET. Individuals used in this analysis included all MCSA participants (CN, MCI, and AD dementia) with at least one follow-up imaging study.

The specificity-based cut-point corresponded to the 95th percentile of the biomarker distribution among MCSA CN individuals’ ages 30-49 years, all of whom were amyloid negative based on the reliable worsening cut-point described above. As noted above, we treat all biomarkers such that the 95th percentile corresponds to more abnormal values. The rationale for a specificity-based cut-point is that young individuals are likely to be relatively free of AD pathology. This approach is commonly used in laboratory medicine [40]. This approach was applicable to all 4 imaging methods. Because of limited sample sizes among those with tau PET, we estimated the 95th percentile based on calculating a smoothed

cumulative distribution function (CDF) from a kernel density estimate of the distribution. This can be interpreted as a smoothed empirical CDF.

The sensitivity-based cut-point corresponded to the 10th percentile of the biomarker distribution among cognitively impaired (aMCI or AD) individuals from the MCSA or ADRC aged 60 or older who were amyloid positive, where the definition of amyloid positivity was based on the reliable worsening cut-point described above. The 10th percentile (i.e., 90% sensitivity) in this impaired group was calculated using the same CDF approach described above. This method is very similar to our earlier approach from 2012 [16]. However, this updated method only included amyloid positive people so that the clinically impaired group was not contaminated with individuals who are not in the AD pathway [17]. This sensitivity-based cut-point is only applicable to selecting the cut-point for MRI, FDG PET, and tau PET because the impaired group was required to have elevated values of amyloid PET.

The fourth method was based on discriminating between the cognitively impaired individuals used in the sensitivity cut-point analysis and younger CN individuals used in the specificity cut-point analysis. This case/control discrimination cut-point was obtained by identifying the point of maximum separation between the smoothed CDFs of the two groups. This is equivalent to maximizing accuracy, defined as sensitivity - (1 - specificity). This method is only applicable to selecting cut-points for MRI, FDG PET, and tau PET because the clinically impaired individuals were required to have elevated amyloidosis.

The fifth method was also based on discriminating between cognitively impaired and CN individuals. However, in contrast to the fourth method, the control group consisted of older amyloid negative CN individuals from the MCSA who were age- and sex-matched to the impaired group. Using a control group with similar ages as the cognitively impaired group allows this cut-point to focus on AD-related differences between the groups as opposed to both AD- and non-specific age-related differences. Requiring the CN individuals to be amyloid negative insures that controls are not in the AD pathway. This method is only applicable to selecting cut-points for MRI, FDG PET, and tau PET because amyloid PET was used to define both groups.

2.4.2. Methods for evaluating cut-points—To evaluate the utility of cut-points defined from the different methods above, we estimated the proportion of MCSA CN individuals with abnormal biomarker values by age using logistic regression models. Age was fit with a restricted cubic spline with knots at ages 50, 65, and 80. We also generated histograms of the biomarkers among all MCSA individuals aged 50-89 to illustrate where the cut-points fall in the biomarker distributions within a population. These histograms were weighted to reflect the age/sex frequencies in Olmsted County.

3. Results

Characteristics of the clinical groups used are found in Table 1**,** where we distinguish between the two samples in our study. Supplementary Fig. 1 illustrates how the clinical

groups within the tau/amyloid/MRI sample compare to the clinical groups in the amyloid/FDG/MRI sample.

Fig. 2 shows the relationship between the annual rate of change and baseline biomarker for amyloid PET, FDG PET, and cortical thickness among all MCSA individuals with serial imaging. Tau PET is not shown because we only have cross-sectional data currently. Using this reliable worsening method, we defined the amyloid PET cut-point as 1.42 SUVR, corresponding to a centiloid value of 19. A reliable worsening cut-point could not be determined for FDG or cortical thickness because the rate of change was not associated with the baseline biomarker values

Fig. 3 shows the estimated cumulative distribution function among younger CN individuals, cognitively impaired individuals, and age- and sex-matched CN individuals. The specificity, sensitivity, and accuracy of impaired versus younger CN methods gave very similar cut-points within each biomarker: 1.19, 1.21, and 1.21 SUVR for tau PET, respectively; 1.55, 1.56, and 1.56 SUVR for FDG PET; and 2.69, 2.70, and 2.67 mm for cortical thickness. However, cut-points defined using the accuracy of impaired versus age-matched CN method were always more conservative (1.32 SUVR for tau PET, 1.42 SUVR for FDG PET, and 2.57 mm for cortical thickness). While a cut-point for amyloid PET could not be determined using the sensitivity or accuracy methods due to circularity in group definitions, the specificity method produced a cut-point of 1.26 SUVR, centiloid 5.

In Fig. 4**,** we illustrate the continuous distribution of amyloid PET, tau PET, FDG PET, and MRI cortical thickness values versus age among all MCSA CN with horizontal lines representing the cut-points from each method. A box plot of values among impaired individuals is included in the plot of each biomarker for reference.

Fig. 4 also shows the estimated proportion of CN that are labeled positive (abnormal) by age for each of the five cut-point methods. For tau PET, the cut-point from the specificity method labeled the most people positive, while the sensitivity and accuracy of impaired versus young CN methods (which were the same) labeled about 10% fewer people positive. For FDG PET, these three methods performed essentially identically. Performance was similar across the three methods for cortical thickness, although the sensitivity method labelled more people positive and the accuracy of impaired CN fewer by roughly 10%. In contrast, cut-points defined using the accuracy of impaired versus age-matched CN method labeled the fewest people positive for all biomarkers. For example, at age 70 the proportion of CN labeled positive using the specificity, sensitivity, accuracy of impaired versus young CN, and accuracy of impaired versus age-matched CN methods for tau PET is 46%, 33%, 33%, and 6%, respectively. For FDG PET, the proportions were 42%, 44%, 44%, and 10% and for MRI cortical thickness the proportions were 37%, 41%, 31%, and 10%. For amyloid PET, 29% of CN individuals are labeled positive at age 70 using the reliable worsening cut-point, in contrast to 89% using the specificity cut-point.

In Fig. 5**,** we illustrate the histograms of the distribution of values among all MCSA individuals ages 50-89 along with the cut-points selected by the different methods for each. The histograms have been weighted by age and sex to reflect the age/sex population

frequencies in Olmsted County. We also show the distribution of a prototypical non-imaging and non-AD biomarker, systolic blood pressure, to illustrate how an established biomarker and its accepted cut-point compares with those used in AD research. MRI, FDG PET, tau PET, and systolic blood pressure are all approximately normally distributed. The frequency distribution of amyloid PET is unimodal but has a prominent skew.

Supplementary Fig. 2 illustrates how the proportion of MCSA CN individuals labeled positive by age using the cut-point definitions for amyloid PET, FDG PET, and MRI cortical thickness defined in this analysis compare to our previous cut-point definitions [41].

4. Discussion

4.1. Cut-point selection for amyloid PET

Of the five cut-point methods considered, only the reliable worsening and specificity methods are applicable to amyloid PET, since amyloid positivity was used in the group definitions for the other methods. However, the specificity cut-point of SUVR 1.26, centiloid 5, classifies 89% of CN individuals in the MCSA at age 70 as amyloid positive. A cut-point indicating most 70 year olds are amyloid positive is inconsistent with autopsy data which indicate that the proportion of the population with amyloidosis at age 70 is just under 40% [42]. Therefore, the cut-point obtained from the sensitivity method is not plausible for amyloid PET because *in vivo* imaging methods should be less sensitive than direct examination of tissue at autopsy.

Selecting a cut-point based on a threshold value beyond which the rate of change in that biomarker worsens reliably has high face validity. It is a particularly useful approach for amyloid because the properties of the biomarker itself are used to select the cut-point, independent from any relationship to clinical symptoms [43-46]. The amyloid PET cut-point selected by this reliable worsening method of 1.42 SUVR is similar to the 1.40 SUVR we used in the past, although we made some changes to the implementation of amyloid PET quantitative pipeline. These include no partial volume correction and a slightly different cerebellar reference ROI. Nonetheless, our old and new amyloid cut-points labelled very similar proportions of the MCSA population as positive across all ages (Supplementary Fig. 2). An SUVR of 1.40 with our old method corresponded to Thal phase < 2 in our imaging-autopsy analysis [14]. Thus, 1.42 SUVR with our new method seems to be a well determined cut-point for amyloid PET.

SUVR values are laboratory specific units that depend on the tracer used and the methodological implementation of data processing. The centiloid concept was introduced for amyloid PET to enable the field to express quantitative amyloid PET in universal units. A cut-point of 1.42 SUVR with our current data processing methods corresponds to a centiloid value of 19.

4.2. Approach to Tau PET quantification

We selected the entorhinal, amygdala, parahippocampal, fusiform, inferior temporal, and middle temporal ROIs for our tau meta-ROI because ligand uptake appears first in medial temporal ROIs in clinically normal individuals with advancing age [27-29, 31]. Ligand

uptake in basal/lateral temporal lobe— fusiform, inferior temporal, and middle temporal — is associated with characteristics of AD such as amyloid positivity, worse cognitive performance in CN individuals, and the clinical diagnosis of MCI or AD dementia [27-31]. Temporal lobe tau PET uptake also predicts elevated (abnormal) CSF tau [30]. Thus, this composite set of ROIs captures a broad dynamic range across the normal to pathological aging to AD dementia spectrum [30]. We did not include the hippocampus in the tau PET meta-ROI because of frequent bleed-in from off-target uptake in the choroid plexus.

An argument can be made that tau PET should be reported in stages analogously to Braak stage [29, 47] rather than using a binary positive/negative designation. However, a tau PET quantification method based on the magnitude of uptake in an AD signature composite-ROI that captures a broad diagnostic range, as reported in this study, encapsulates the concept of pathological severity. Furthermore, every test used in medicine has some notion of a positive/negative cut-point in its continuous distribution, and an effort to accomplish the same for tau PET seems logical.

4.3. Selecting cut-points for tau PET, FDG PET and MRI

For MRI and FDG PET, there was no clear evidence of a threshold value beyond which rates of hypometabolism or cortical thinning increase. Thus, the reliable worsening method did not produce a cut-point for FDG PET or MRI (Fig. 2). As noted above, with no serial data, a reliable worsening cut-point for tau PET could not be obtained. Using the other cut-point methods of specificity, sensitivity, and accuracy of cognitively impaired versus young CN produced more lenient cut-points while the accuracy of cognitively impaired versus age-matched CN method produced more conservative cut-points.

The fact that several of the cut-point methods produced very consistent results for tau PET, FDG PET, and MRI lends support to the validity of these more lenient cut-points. We emphasize that regardless of how lenient or conservative a cut-point is, if an individual falls below that cut-point for a particular biomarker this does not imply that no pathology is present in the brain. An individual labeled negative may well have pathology in the brain, but not at a sufficient level to cross the *in vivo* detection threshold of the biomarker in question.

4.4. Dispelling myths about cut-points

Examination of the data in Fig. 5 should challenge several popular assumptions about AD biomarkers. The first is that amyloid PET (and CSF Ab42) are bimodally distributed in “the population” [48]. While that is true in highly selected samples composed mostly of impaired individuals [48], it is not true in our population-based sample where most are not demented (Fig. 5**)**. A second assumption is that cut-points for any AD biomarker other than amyloid are not valid because these biomarkers are not bimodally distributed. The distribution of systolic blood pressure in Fig. 5 illustrates an example of one of many established biomarker that is approximately normally distributed and has a cut-point that is widely used clinically.

Supplementary Material

Refer to Web version on PubMed Central for supplementary material.

Acknowledgements

This study was supported by the National Institute of Health (R01 AG011378, R01 AG041851, U01 AG006786, R01 AG034676) and the Alexander Family Alzheimer's Disease Research Professorship of the Mayo Foundation.

References

[1]. Sperling RA, Rentz DM, Johnson KA, Karlawish J, Donohue M, Salmon DP, et al. The A4 study: stopping AD before symptoms begin? Sci Transl Med. 2014; 6:228fs13.

[2]. Hampel H, Schneider LS, Giacobini E, Kivipelto M, Sindi S, Dubois B, et al. Advances in the therapy of Alzheimer's disease: targeting amyloid beta and tau and perspectives for the future. Expert Rev Neurother. 2015; 15:83–105. [PubMed: 25537424]

[3]. Dubois B, Feldman HH, Jacova C, Hampel H, Molinuevo JL, Blennow K, et al. Advancing research diagnostic criteria for Alzheimer's disease: the IWG-2 criteria. Lancet Neurol. 2014; 13:614–29. [PubMed: 24849862]

[4]. Albert MS, DeKosky ST, Dickson D, Dubois B, Feldman HH, Fox NC, et al. The diagnosis of mild cognitive impairment due to Alzheimer's disease: Recommendations from the National Institute on Aging and Alzheimer's Association Workgroup. Alzheimers Dement. 2011; 7:270–9. [PubMed: 21514249]

[5]. Jack CR Jr. Albert MS, Knopman DS, McKhann GM, Sperling RA, Carillo M, et al. Introduction to the recommendations from the National Institute on Aging-Alzheimer's Association workgroups on diagnostic guidelines for Alzheimer's disease. Alzheimers Dement. 2011; 7:257–62. [PubMed: 21514247]

[6]. McKhann GM, Knopman DS, Chertkow H, Hyman BT, Jack CR Jr. Kawas CH, et al. The diagnosis of dementia due to Alzheimer's disease: Recommendations from the National Institute on Aging and the Alzheimer's Assocation Workgroup. Alzheimers Dement. 2011; 7:263–9. [PubMed: 21514250]

[7]. Sperling RA, Aisen PS, Beckett LA, Bennett DA, Craft S, Fagan AM, et al. Toward defining the preclinical stages of Alzheimer's disease: recommendations from the National Institute on Aging-Alzheimer's Assocation workgroups on diagnostic guidelines for Alzheimer's disease. Alzheimers Dement. 2011; 7:280–92. [PubMed: 21514248]

[8]. Mormino EC, Brandel MG, Madison CM, Rabinovici GD, Marks S, Baker SL, et al. Not quite PIB-positive, not quite PIB-negative: Slight PIB elevations in elderly normal control subjects are biologically relevant. Neuroimage. 2012; 59:1152–60. [PubMed: 21884802]

[9]. Villeneuve S, Rabinovici GD, Cohn-Sheehy BI, Madison C, Ayakta N, Ghosh PM, et al. Existing Pittsburgh Compound-B positron emission tomography thresholds are too high: statistical and pathological evaluation. Brain. 2015; 138:2020–33. [PubMed: 25953778]

[10]. Pike KE, Savage G, Villemagne VL, Ng S, Moss SA, Maruff P, et al. Beta-amyloid imaging and memory in non-demented individuals: evidence for preclinical Alzheimer's disease. Brain. 2007; 130:2837–44. [PubMed: 17928318]

[11]. Rowe CC, Ellis KA, Rimajova M, Bourgeat P, Pike KE, Jones G, et al. Amyloid imaging results from the Australian Imaging, Biomarkers and Lifestyle (AIBL) study of aging. Neurobiol Aging. 2010; 31:1275–83. [PubMed: 20472326]

[12]. Hedden T, Van Dijk KR, Becker JA, Mehta A, Sperling RA, Johnson KA, et al. Disruption of functional connectivity in clinically normal older adults harboring amyloid burden. J Neurosci. 2009; 29:12686–94. [PubMed: 19812343]

[13]. Villemagne VL, Pike KE, Chetelat G, Ellis KA, Mulligan RS, Bourgeat P, et al. Longitudinal assessment of Abeta and cognition in aging and Alzheimer disease. Ann Neurol. 2011; 69:181–92. [PubMed: 21280088]

[14]. Murray ME, Lowe VJ, Graff-Radford NR, Liesinger AM, Cannon A, Przybelski SA, et al. Clinicopathologic and 11C-Pittsburgh compound B implications of Thal amyloid phase across the Alzheimer's disease spectrum. Brain. 2015; 138:1370–81. [PubMed: 25805643]

[15]. Thal DR, Beach TG, Zanette M, Heurling K, Chakrabarty A, Ismail A, et al. [(18)F]flutemetamol amyloid positron emission tomography in preclinical and symptomatic Alzheimer's disease:

Specific detection of advanced phases of amyloid-beta pathology. Alzheimers Dement. 2015; 11:975–85. [PubMed: 26141264]

[16]. Jack CR Jr. Knopman DS, Weigand SD, Wiste HJ, vemuri P, Lowe V, et al. An operational approach to NIA-AA crtiteria for preclinical Alzheimer's disease. Ann Neurol. 2012; 71:765–75. [PubMed: 22488240]

[17]. Wisse LE, Butala N, Das SR, Davatzikos C, Dickerson BC, Vaishnavi SN, et al. Suspected non-AD pathology in mild cognitive impairment. Neurobiol Aging. 2015; 36:3152–62. [PubMed: 26422359]

[18]. Beach TG, Monsell SE, Phillips LE, Kukull W. Accuracy of the clinical diagnosis of Alzheimer disease at National Institute on Aging Alzheimer Disease Centers, 2005-2010. J Neuropathol Exp Neurol. 2012; 71:266–73. [PubMed: 22437338]

[19]. Salloway S, Sperling R, Fox NC, Blennow K, Klunk W, Raskind M, et al. Two phase 3 trials of bapineuzumab in mild-to-moderate Alzheimer's disease. N Engl J Med. 2014; 370:322–33. [PubMed: 24450891]

[20]. Ossenkoppele R, Jansen WJ, Rabinovici GD, et al. Prevalence of amyloid pet positivity in dementia syndromes: A meta-analysis. JAMA. 2015; 313:1939–49. [PubMed: 25988463]

[21]. Knopman DS, Parisi JE, Salviati A, Floriach-Robert M, Boeve BF, Ivnik RJ, et al. Neuropathology of cognitively normal elderly. J Neuropathol Exp Neurol. 2003; 62:1087–95. [PubMed: 14656067]

[22]. Aizenstein HJ, Nebes RD, Saxton JA, Price JC, Mathis CA, Tsopelas ND, et al. Frequent amyloid deposition without significant cognitive impairment among the elderly. Arch Neurol. 2008; 65:1509–17. [PubMed: 19001171]

[23]. Jansen WJ, Ossenkoppele R, Knol DL, et al. Prevalence of cerebral amyloid pathology in persons without dementia: A meta-analysis. JAMA. 2015; 313:1924–38. [PubMed: 25988462]

[24]. Mielke MM, Wiste HJ, Weigand SD, Knopman DS, Lowe VJ, Roberts RO, et al. Indicators of amyloid burden in a population-based study of cognitively normal elderly. Neurology. 2012; 79:1570–7. [PubMed: 22972644]

[25]. Villemagne VL, Fodero-Tavoletti MT, Masters CL, Rowe CC. Tau imaging: early progress and future directions. The Lancet Neurology. 2015; 14:114–24. [PubMed: 25496902]

[26]. Villemagne VL, Furumoto S, Fodero-Tavoletti MT, Mulligan RS, Hodges J, Harada R, et al. In vivo evaluation of a novel tau imaging tracer for Alzheimer's disease. Eur J Nucl Med Mol Imaging. 2014; 41:816–26. [PubMed: 24514874]

[27]. Johnson KA, Shultz A, Betensky RA, Becker JA, Sepulcre J, Rentz DM, et al. Tau positron emission tomographic imaging in aging and early Alzheimer's disease. Ann Neurol. 2016; 79:110–9. [PubMed: 26505746]

[28]. Scholl M, Lockhart SN, Schonhaut DR, O'Neil JP, Janabi M, Ossenkoppele R, et al. PET Imaging of tau deposition in the aging human brain. Neuron. 2016; 89:971–82. [PubMed: 26938442]

[29]. Schwarz AJ, Yu P, Miller BB, Shcherbinin S, Dickson J, Navitsky M, et al. Regional profiles of the candidate tau PET ligand 18F-AV-1451 recapitulate key features of Braak histopathological stages. Brain. 2016 Epub ahead of print.

[30]. Brier MR, Gordon B, Friedrichsen K, McCarthy J, Stern A, Christensen J, et al. Tau and Aβ imaging, CSF measures, and cognition in Alzheimer's disease. Sci Transl Med. 2016; 8:338ra66–ra66.

[31]. Lowe, V., Wiste, HJ., Pandey, M., Senjem, M., Boeve, B., Josephs, KA., et al. Tau-PET imaging with AV-1451 in Alzheimer's disease. In: Johnson, KA.Jagust, W.Klunk, W., Mathis, C., editors. Human Amyloid Imaging. Miami Beach, FL: 2016. p. 114

[32]. Klunk, WE., Cohen, A., Bi, W., Weissfeld, L., Aizenstein, H., McDade, E., et al. Why we need two cutoffs for amyloid-imaging: Early versus Alzheimer's-like amyloid-positivity; Alzheimer's Association International Conference; Vancouver, British Columbia, Canada: Alzheimer's Associaton. 2012; p. P453-P4.

[33]. Bartlett JW, Frost C, Mattsson N, Skillback T, Blennow K, Zetterberg H, et al. Determining cut-points for Alzheimer's disease biomarkers: statistical issues, methods and challenges. Biomark Med. 2012; 6:391–400. [PubMed: 22917141]

[34]. Roberts RO, Geda YE, Knopman DS, Cha RH, Pankratz VS, Boeve BF, et al. The Mayo Clinic Study of Aging: design and sampling, participation, baseline measures and sample characteristics. Neuroepidemiology. 2008; 30:58–69. [PubMed: 18259084]

[35]. Klunk WE, Engler H, Nordberg A, Wang Y, Blomqvist G, Holt DP, et al. Imaging brain amyloid in Alzheimer's disease with Pittsburgh Compound-B. Ann Neurol. 2004; 55:306–19. [PubMed: 14991808]

[36]. Senjem ML, Gunter JL, Shiung MM, Petersen RC, Jack CR Jr. Comparison of different methodological implementations of voxel-based morphometry in neurodegenerative disease. Neuroimage. 2005; 26:600–8. [PubMed: 15907317]

[37]. Klunk WE, Koeppe RA, Price JC, Benzinger T, Devous M, Jagust W, et al. The Centiloid Project: Standardizing quantitative amyloid plaque estimation by PET. Alzheimer's & dementia. 2015; 11:1–15.

[38]. Landau SM, Harvey D, Madison CM, Koeppe RA, Reiman EM, Foster NL, et al. Associations between cognitive, functional, and FDG-PET measures of decline in AD and MCI. Neurobiol Aging. 2011; 32:1207–18. [PubMed: 19660834]

[39]. Villain N, Chetelat G, Grassiot B, Bourgeat P, Jones G, Ellis KA, et al. Regional dynamics of amyloid-beta deposition in healthy elderly, mild cognitive impairment and Alzheimer's disease: a voxelwise PiB-PET longitudinal study. Brain. 2012; 135:2126–39. [PubMed: 22628162]

[40]. Grasbeck R. The evolution of the reference value concept. Clin Chem Lab Med. 2004; 42:692–7. [PubMed: 15327001]

[41]. Jack CR, Wiste HJ, Weigand S, Knopman D, Mielke MM, Vemuri P, et al. Different definitions of neurodegeneration produce similar frequencies of amyloid and neurodegeneration biomarker groups by age among cognitively non-impaired individuals. Brain. 2015

[42]. Braak H, Thal DR, Ghebremedhin E, Del Tredici K. Stages of the pathologic process in Alzheimer disease: age categories from 1 to 100 years. J Neuropathol Exp Neurol. 2011; 70:960–9. [PubMed: 22002422]

[43]. Ingelsson M, Fukumoto H, Newell KL, Growdon JH, Hedley-Whyte ET, Frosch MP, et al. Early Abeta accumulation and progressive synaptic loss, gliosis, and tangle formation in AD brain. Neurology. 2004; 62:925–31. [PubMed: 15037694]

[44]. Mormino EC, Kluth JT, Madison CM, Rabinovici GD, Baker SL, Miller BL, et al. Episodic memory loss is related to hippocampal-mediated beta-amyloid deposition in elderly subjects. Brain. 2009; 132:1310–23. [PubMed: 19042931]

[45]. Jack CR Jr. Lowe VJ, Weigand SD, Wiste HJ, Senjem ML, Knopman DS, et al. Serial PIB and MRI in normal, mild cognitive impairment and Alzheimer's disease: implications for sequence of pathological events in Alzheimer's disease. Brain. 2009; 132:1355–65. [PubMed: 19339253]

[46]. Perrin RJ, Fagan AM, Holtzman DM. Multimodal techniques for diagnosis and prognosis of Alzheimer's disease. Nature. 2009; 461:916–22. [PubMed: 19829371]

[47]. Braak H, Braak E. Neuropathological stageing of Alzheimer-related changes. Acta Neuropathol. 1991; 82:239–59. [PubMed: 1759558]

[48]. De Meyer G, Shapiro F, Vanderstichele H, Vanmechelen E, Engelborghs S, De Deyn PP, et al. Diagnosis-Independent Alzheimer Disease Biomarker Signature in Cognitively Normal Elderly People. Arch Neurol. 2010; 67:949–56. [PubMed: 20697045]

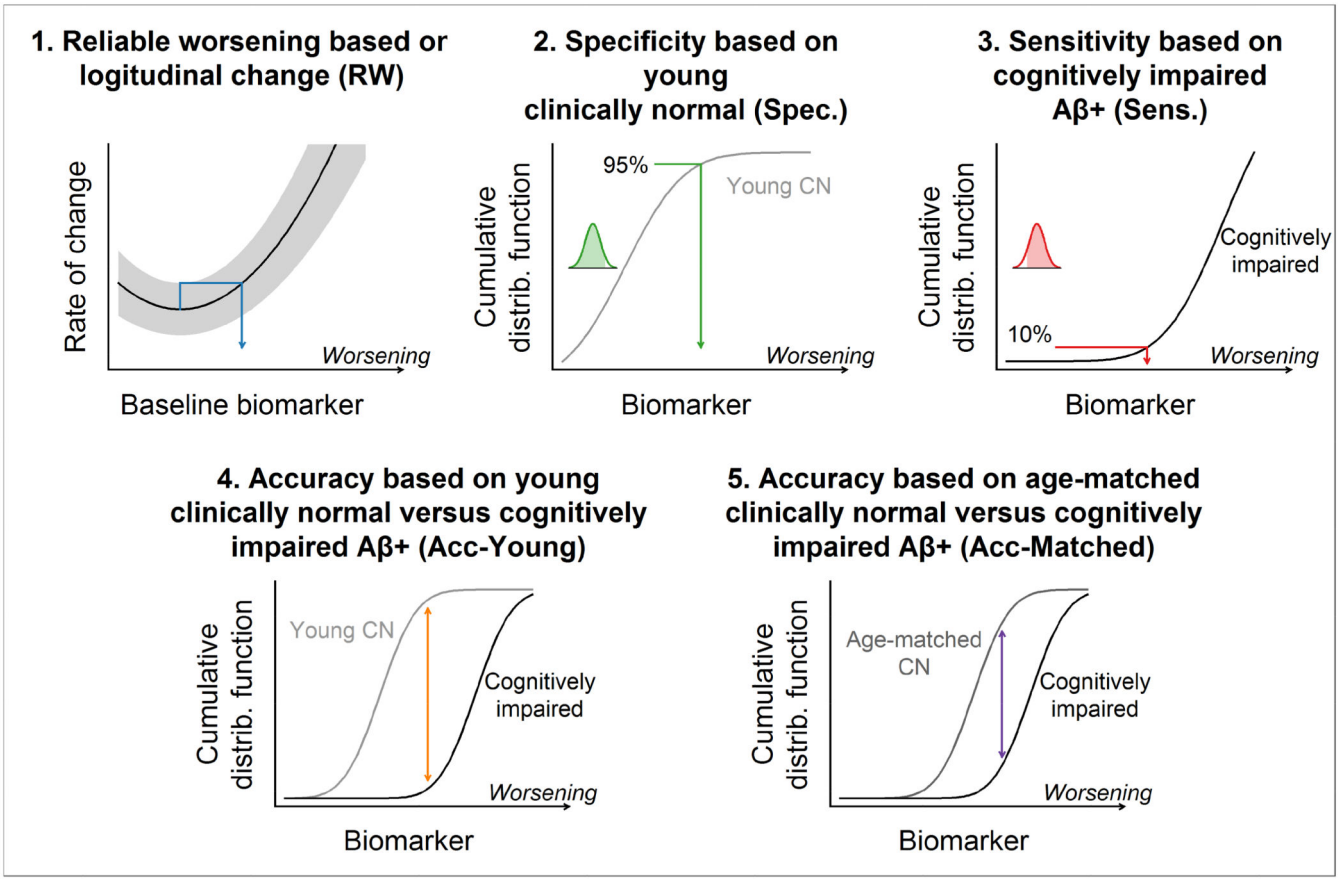

Figure 1. Cut-point methods

Graphical summary of the five methods used for determining cut-points. In each panel, increasing numeric values of the biomarker correspond to biomarker worsening. A biomarker's cumulative distribution function (CDF) indicates a biomarker value x on the horizontal axis and the proportion of observations less than or equal x on the vertical axis.

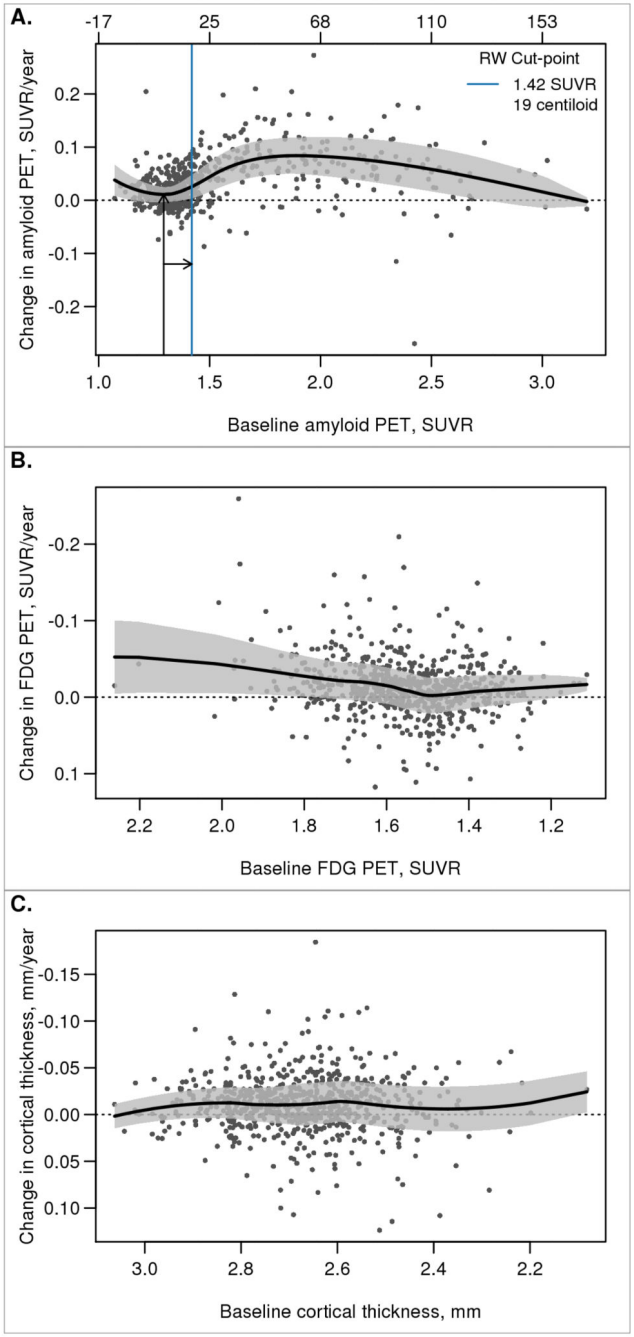

Figure 2. Reliable worsening cut-point

Scatter plot of annual rate of change in imaging biomarker versus baseline with a nonparametric scatter plot smoother line and a 50% prediction interval. For amyloid PET (panel A), the arrows and solid blue line illustrate how the reliable worsening (RW) cut-point was obtained. For this panel, values are shown in both SUVR and centiloid units. A reliable worsening cut-point was not obtained for FDG PET or MRI cortical thickness (panels B and C).

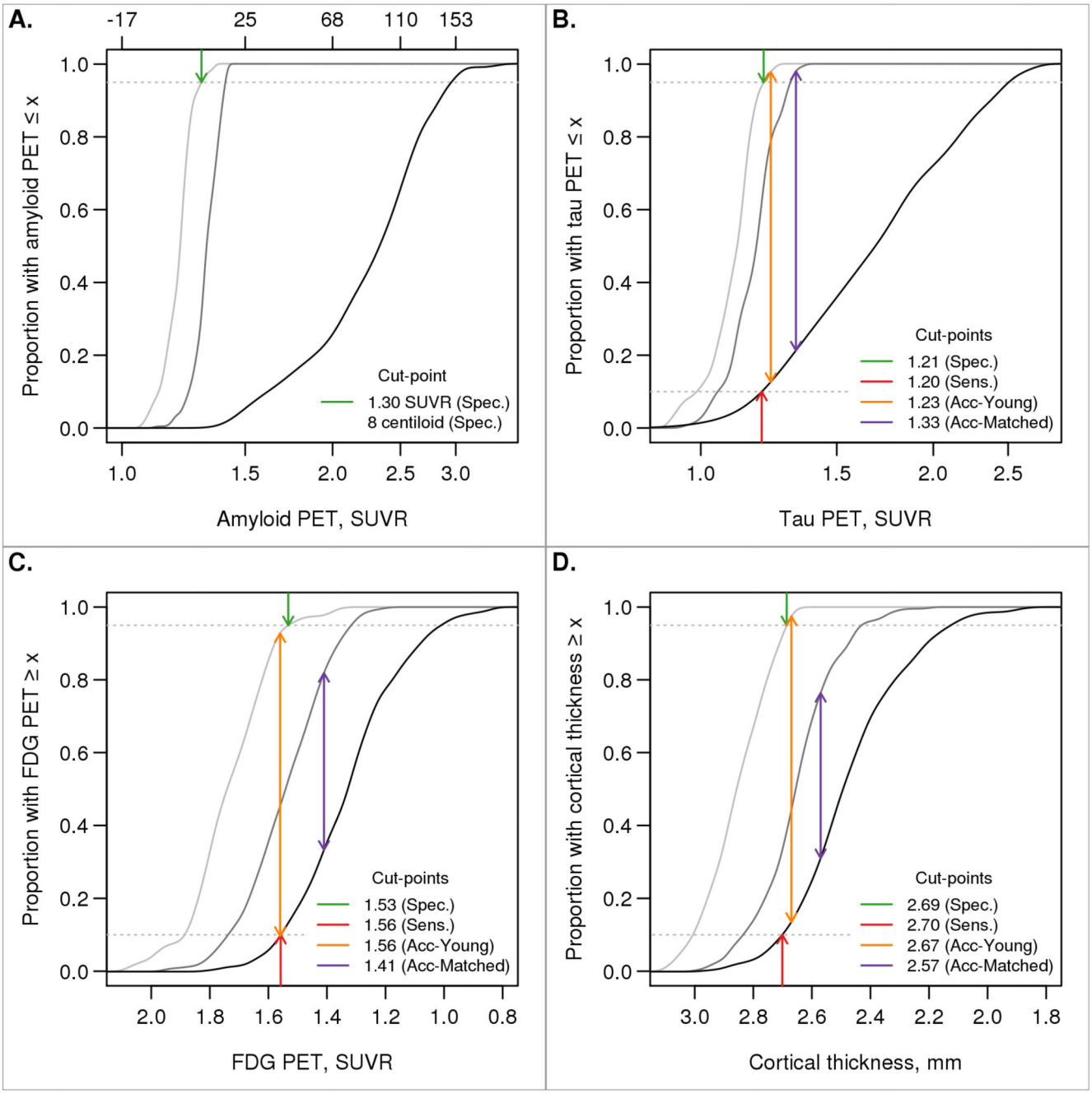

Figure 3. Specificity, sensitivity, and accuracy cut-points

Cumulative distribution function (CDF) plots for young CN individuals (light grey), cognitively impaired individuals (black), and older CN individuals that were age- and sex-matched to the cognitively impaired group (dark grey). The arrows indicate cut-points chosen corresponding to 95% specificity (CDF = 0.95, dark green arrow), 90% sensitivity (CDF = 0.10, dark red arrow), accuracy in discriminating between young CN and cognitively impaired individuals (orange arrow), and accuracy in discriminating between age-matched CN and cognitively impaired individuals (purple arrow). Accuracy was defined

as the point of maximum difference between two CDFs. Amyloid PET was used in the definition of the cognitively impaired group so only the specificity cut-point is shown. For amyloid PET (panel A), values are shown in both SUVR and centiloid units.

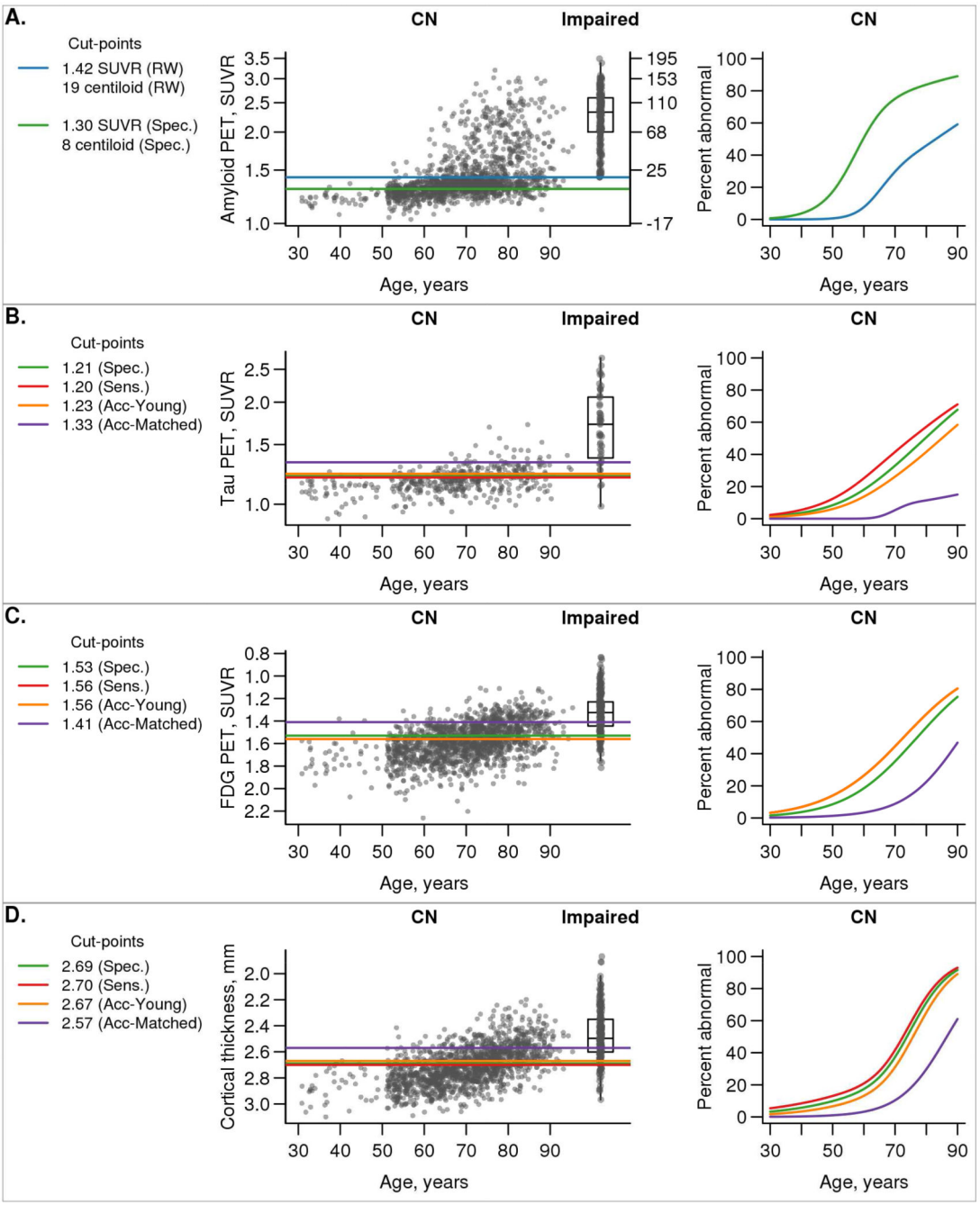

Figure 4. Biomarkers vs age

Scatter plots of each biomarker versus age among all MCSA CN individuals with box plots of the cognitively impaired group shown for reference. The horizontal lines indicate cut-points chosen from the five methods. The colors used were as follows: reliable worsening (RW), blue (only in panel A); specificity (Spec.), green; sensitivity (Sens.), red; accuracy of cognitively impaired versus young CN (Acc-Young), orange; accuracy of cognitively impaired versus matched CN (Acc-Matched), purple. Using each of these five cut-point methods, we then label individuals as positive or negative and show the percent positive as

estimated from logistic regression models. For amyloid PET (panel A), values are shown in both SUVR and centiloid units.

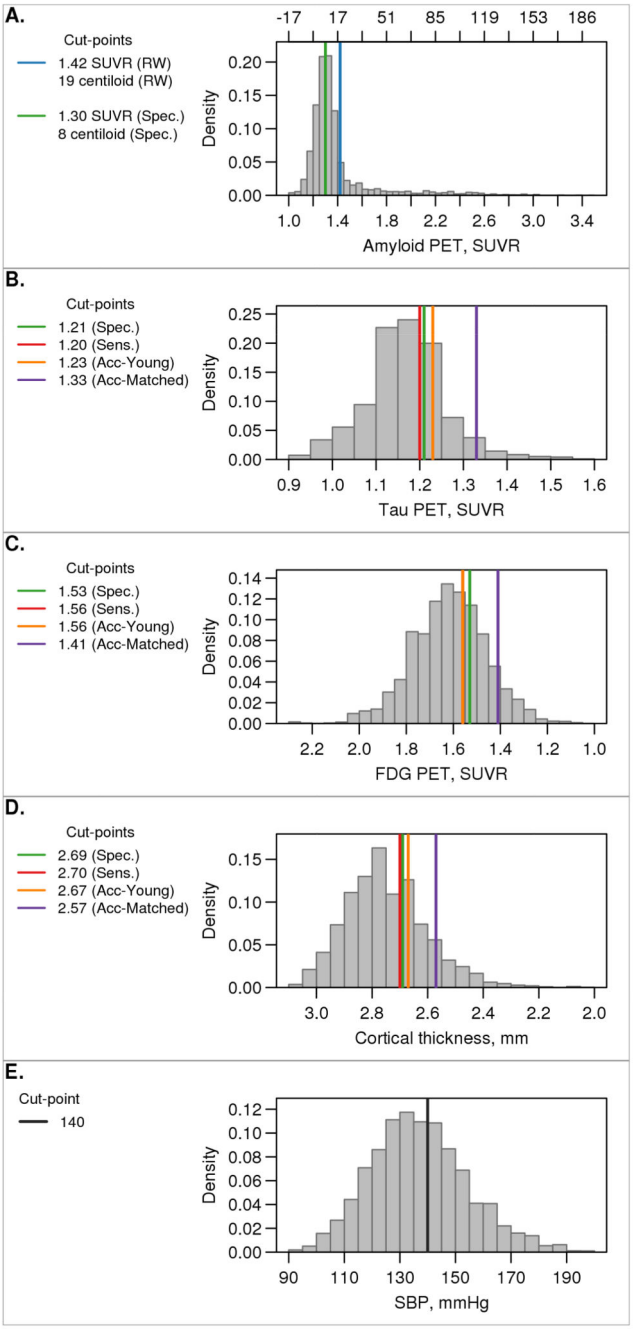

Figure 5. Distribution of biomarkers in MCSA sample

Histograms of the distribution of each biomarker (panels A-D) among all MCSA individuals aged 50-89 weighted to the Olmsted County population by age and sex. The horizontal lines indicate cut-points chosen from the five methods. The colors used were as follows: reliable worsening (RW), blue (panel A only); specificity (Spec.), green; sensitivity (Sens.), red; accuracy of cognitively impaired versus young CN (Acc-Young), orange; accuracy of cognitively impaired versus matched CN (Acc-Matched), purple. Systolic blood pressure is

also shown in panel E with the cut-point of 140 mmHg (black line). For amyloid PET (panel A), values are shown in both SUVR and centiloid units.

Table 1

Characteristics of participant samples used in analyses

Characteristic	Tau/Amyloid/MRI Sample					Amyloid/FDG/MRI Sample				
	Cut-point definition samples			Cut-point evaluation samples		Cut-point definition samples			Cut-point evaluation samples	
	Young CN (n=49)	Matched CN* (n=102)	Cognitively impaired† (n=51)	All CN (n=438)	MCSA 50-89‡ (n=417)	Matched CN* (n=214)	Cognitively impaired† (n=214)	MCSA Serial§ (n=682)	All CN (n=1503)	MCSA 50-89‡ (n=1646)
Age, years										
Median (IQR)	39 (34, 44)	73 (67, 78)	74 (67, 79)	69 (59, 78)	71 (64, 79)	77 (72, 84)	77 (72, 84)	75 (68, 80)	71 (63, 78)	72 (64, 79)
Min, Max	30, 48	60, 90	60, 88	30, 94	52, 89	60, 93	60, 93	51, 94	30, 95	50, 89
Male gender, no. (%)	28 (57%)	70 (69%)	35 (69%)	241 (55%)	236 (57%)	124 (58%)	124 (58%)	399 (59%)	790 (53%)	882 (54%)
Education, years, Median (IQR)	16 (14, 16)	14 (13, 17)	16 (12, 16)	16 (13, 17)	15 (13, 16)	14 (12, 17)	15 (12, 16)	14 (12, 16)	15 (12, 16)	14 (12, 16)
APOE ε4 positive, no. (%)	5 (19%)	15 (15%)	33 (72%)	106 (26%)	109 (27%)	29 (14%)	143 (69%)	187 (28%)	392 (27%)	462 (29%)
MMSE, Median (IQR)	29 (29, 30)	29 (28, 29)	24 (22, 27)	29 (28, 29)	29 (28, 29)	28 (27, 29)	25 (22, 27)	28 (27, 29)	29 (28, 29)	29 (27, 29)
Tau PET, SUVR, Median (IQR)	1.12 (1.06, 1.14)	1.18 (1.11, 1.22)	1.72 (1.37, 2.07)	1.18 (1.12, 1.23)	1.19 (1.13, 1.25)					
Amyloid PET, SUVR, Median (IQR)	1.21 (1.17, 1.24)	1.32 (1.28, 1.37)	2.50 (2.24, 2.70)	1.35 (1.27, 1.48)	1.36 (1.29, 1.53)	1.32 (1.29, 1.37)	2.33 (2.00, 2.59)	1.36 (1.30, 1.54)	1.34 (1.28, 1.45)	1.35 (1.29, 1.51)
FDG PET, SUVR, Median (IQR)	1.74 (1.65, 1.82)	1.54 (1.46, 1.64)	1.20 (1.12, 1.34)	1.57 (1.47, 1.66)	1.54 (1.45, 1.64)	1.54 (1.44, 1.64)	1.32 (1.23, 1.44)	1.55 (1.45, 1.65)	1.58 (1.47, 1.68)	1.56 (1.45, 1.66)
Cortical thickness, mm, Median (IQR)	2.86 (2.78, 2.93)	2.70 (2.60, 2.79)	2.39 (2.27, 2.60)	2.73 (2.63, 2.83)	2.70 (2.61, 2.80)	2.65 (2.58, 2.73)	2.50 (2.35, 2.60)	2.67 (2.59, 2.77)	2.71 (2.62, 2.81)	2.70 (2.60, 2.80)

*The matched CN subgroups include clinically normal individuals from the MCSA aged 60 or older with amyloid PET < 1.42 SUVR and are matched on age (within 3 years) and sex to the cognitively impaired subgroups. The Tau/Amyloid/MRI matched CN sample was matched 2 to 1 to the Tau/Amyloid/MRI cognitively impaired sample. The Amyloid/FDG/MRI matched CN sample was matched 1 to 1 to the Amyloid/FDG/MRI cognitively impaired sample

†The Tau/Amyloid/MRI cognitively impaired subgroup includes 19 aMCI and 33 AD dementia individuals with amyloid PET > 1.42 SUVR and aged 60 or older. The Amyloid/FDG/MRI cognitively impaired subgroup includes 136 aMCI and 79 AD dementia individuals with amyloid PET > 1.42 SUVR and aged 60 or older.

‡The Tau/Amyloid/MRI MCSA 50-89 subgroup includes 384 CN, 27 MCI, 5 individuals with dementia, and 1 individual with an other diagnosis. The Amyloid/FDG/MRI MCSA 50-89 subgroup includes 1446 CN, 186 MCI, 12 individuals with dementia, and 2 individuals with an other diagnosis.

§The Amyloid/FDG/MRI serial imaging subgroup includes 606 CN, 75 MCI, and 1 individual with dementia